Contents lists available at ScienceDirect

Colloids and Surfaces A

journal homepage: www.elsevier.com/locate/colsurfa

Shape and orientation of bare silica particles influence their deposition under intermediate ionic strength: A study with QCM–D and DLVO theory

Allan Gomez-Flores[a], Scott A. Bradford[b], Gukhwa Hwang[a], Sowon Choi[a], Meiping Tong[c], Hyunjung Kim[a,*]

[a] Department of Mineral Resources and Energy Engineering, Jeonbuk National University, 567, Baekje-daero, Deokjin-gu, Jeonju, Jeonbuk,54896, Republic of Korea
[b] US Salinity Laboratory, USDA, ARS, Riverside, CA, USA
[c] The Key Laboratory of Water and Sediment Sciences, Ministry of Education,College of Environmental Sciences and Engineering, Peking University, Beijing, 100871, PR China

GRAPHICAL ABSTRACT

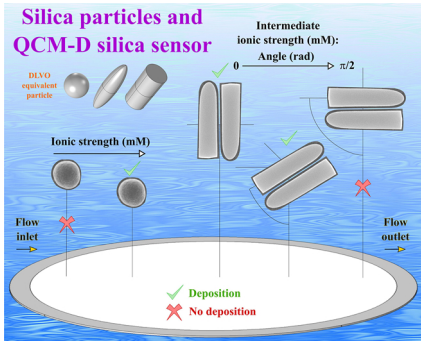

ARTICLE INFO

Keywords:
Silica
QCM – D
DLVO
SEI
Shape
Orientation

ABSTRACT

Theory developed by Derjaguin, Landau, Verwey, and Overbeek (DLVO) is commonly used to interpret and predict the deposition of particles, but it was originally simplified for spherical particles. Many types of bacteria and particles in nature are not spherical. Previous literature has experimentally shown that particle shape has an effect on drug delivery, retention in porous media, self-assembly, and flotation, but the quantitative interpretation of these results has been hindered by experimental (e.g., uniform rod shaped particles and flow fields at controlled chemistries) and theoretical (e.g., consideration of rod shape particles with different surface orientations) challenges. For example, the deposition of ellipsoidal polystyrene particles has been investigated in the presence of non-DLVO interactions, due to residual poly(vinyl) alcohol, hindering the effect of shape. In our study, bare spherical and bullet-like silica particles of well-defined surface chemistry were used for deposition tests on bare silica surfaces using a Quartz Crystal Microbalance with Dissipation (QCM–D) over six ionic strengths (IS). At the same time, the DLVO theory was modified to consider particle shape and orientation of deposition. We found that particle shape had an effect on deposition at intermediate IS. A modified DLVO approach was able to interpret the deposition of bullet-like silica particles. Specifically, bullet-like silica particles of certain aspect ratio may find angles that minimize repulsive energies and overcome energy barriers so that

* Corresponding author.
E-mail address: kshjkim@jbnu.ac.kr (H. Kim).

https://doi.org/10.1016/j.colsurfa.2020.124921
Received 11 February 2020; Received in revised form 15 April 2020; Accepted 24 April 2020
Available online 28 April 2020
0927-7757/

deposition on the silica surfaces is energetically favorable. Therefore, there are conditions of water chemistry where particle shape and orientation cannot be ignored and their deposition must be systematically investigated.

1. Introduction

The Derjaguin, Landau, Verwey, and Overbeek (DLVO) theory is commonly used in colloid science to calculate interaction energies between colloidal particles and planar surfaces. It can be used to interpret or predict colloidal phenomena such as deposition, aggregation, or heterocoagulation from a physicochemical perspective at the micro-and nano-scales. Mathematically, the DLVO theory consists of equations for the sum of attractive van der Waals (VDW) and repulsive electrostatic double layer (EDL) interactions. Conventional DLVO theory is based on the Derjaguin approximation (DA) technique that assumes all particles are spherical for simplicity, even though many particles are known to be non-spherical. For example, natural and engineered particles are of a myriad of complex geometrical shapes. In most cases, they can be approximated using basic regular or irregular geometries including spheres, cylinders, hollow cylinders, ellipsoids, plates, or prisms. The DA has other limitations such as, to mention one, the distance of interaction is shorter than the radii of curvature of the particle [1,2]. Nevertheless, the DA is extensively used to interpret colloidal phenomena, even for non-spherical particles. Simplified equations for cylinders based on the DA are available in the literature [3] but are limited to that shape and preferential orientations. Some studies [4,5] have implemented have implemented the effective radius according to preferential particle orientations (only 0 and $\pi/2$ rad) in the DA to interpret colloidal phenomena of rod-like particles. However, the accurate consideration of particle curvature for non-spherical particles (explicit geometry) and the different orientations during interaction is a complex task using the DA. Thus, systematic investigation of particle shape and orientation using the DA is not available in the literature.

It is important to advance experimental knowledge on the effect of particle shape to obtain accurate data to evaluate interaction energy predictions. Substantial number of studies have experimentally demonstrated that particle shape influences colloidal phenomena at nano- and micro-scales. These studies comprise fields and applications such as environmental and geological research (e.g., fate, transport and retention of colloids [5–9]), self-assembly [10], medical science (e.g., delivering of antibody-coated nanoparticles to lung and brain endothelium [11]), catalysis and energy storage [12], porous composites [13], material science [14], and flotation (e.g., only at low or no collector concentration [15–17]). Furthermore, it has been reported that ellipsoidal colloids and bacteria can lead to different degrees of transport and retention [5,7,8,18], aggregation, and deposition [19], and that colloid shape affects the detachment by a moving air-water interface [20]. It has to be noticed that particle attachment onto a surface (particle, organ, etc.) is an important step to fulfill the objective of some of the mentioned applications. However, most of these studies were conducted in systems that substantially hampered the quantitative determination of the sole influence of particle shape; e.g., spatial variations in hydrodynamics, the presence of air-water interfaces, particles that were coated with polymers, and/or particles that contained surface impurities. For example, ellipsoid polystyrene colloids have been employed in studies [8,21] as surrogates for bacterial cells and elongated minerals. However, surface heterogeneities occur on ellipsoidal polystyrene colloids from residual polyvinyl alcohol (PVA) that remains embedded and on the surface after fabrication [8,22–24].

It was stated in previous literature [5,8] that residual PVA on ellipsoidal polystyrene particles should not be ignored because it can have a considerable effect on the particle surface chemistry. For example, residual PVA on ellipsoidal polystyrene particles was reported [22,23] to create an approximately 10 nm thick layer. One study [24] fabricated spherical polystyrene particles with PVA as a steric stabilizer in organic media and characterized them using Fourier Transform Infrared Spectroscopy (FT–IR) measurements. Results showed that PVA tends to locate at the surface of the spherical polystyrene during fabrication. Furthermore, works [5,8,20,21,23] in the literature used the novel method of Ho et al. [22] to fabricate ellipsoidal polystyrene and conducted deposition experiments. Ho et al. [22] pointed out that residual PVA remains on the surface after fabrication. PVA can enhance particle-particle interactions of ellipsoidal polystyrene particles by altering the electrophoretic mobility and possibly the hydrophobicity [8,20]. Thus, it is presently unclear whether differences in observed colloidal phenomena were caused by particle shape or residual PVA. More systematic research in systems with simple hydrodynamics and chemistries is therefore needed to clearly identify the effect of particle shape.

The surface element integration (SEI) [2] method extends DLVO equations to allow consideration of particle shape and orientation. Only a small number of experimental studies [6,8,21] have used the SEI method to interpret the deposition or aggregation of ellipsoidal particles. However, those studies have only considered two angles of orientation (e.g., parallel and perpendicular to the surface). The interaction energy between ellipsoidal particles and surfaces has been theoretically shown to depend on the particle orientation and the solution ionic strength (IS) [2,25]. Similarly, the significant influence of orientation of cylindrical particles with various aspect ratios on interaction energies has been demonstrated [26]. However, experimental verification of these theoretical results remains incomplete due to difficulties in preparing colloids of well-controlled size, shape, and orientation with surfaces, as well as surface chemistry.

The goal of this research is to precisely determine the influence of particle shape on deposition inside a system with well-defined hydrodynamics at several different IS. To this end, we prepared spherical and bullet-like silica (cylinders of low aspect ratio) particles of comparable diameter, well-defined surface chemistry, and high purity. It was not simple to fabricate large amounts (> 10 mg/batch or 10^5 particles/mL of stock solution) of bullet-like silica particles. We therefore worked with small number of batches for the sake of consistency. These silica particles overcame previous experimental limitations of rod or ellipsoidal polystyrene particles that have a non-uniform surface chemistry due to residual PVA, and allowed us to accurately determine the influence of particle shape on deposition. We measured the deposition of the silica particles on a silica surface using a Quartz Crystal Microbalance with Dissipation (QCM–D) that had a uniform flow field. Deposition results were interpreted using the SEI approach that allows consideration of particle shape and orientation, and results demonstrate that both factors were important for some IS conditions. Therefore, the novelty of our study is the fabrication of non-spherical colloids with well-defined surface chemistry, which is important for avoiding any impact from chemical heterogeneity or non-DLVO interactions. The use of these colloids in a well-controlled and simplified system allowed the accurate comparison between experiments and interaction energy calculations to unambiguously determine the influence of particle shape and orientation on deposition.

2. Materials and methods

2.1. Fabrication and characterization of silica particles

Spherical silica particles were fabricated using the Stöber method [27]. In brief, 60 mL of absolute ethanol ($> 99.5\%$, Sigma-Aldrich) and

7 mL of ammonia (25 mass percent in water, Merck Chemicals) were mixed and stirred in a plastic bottle. Next, 1.90 mL of tetraethyl orthosilicate (TEOS 98%, Sigma-Aldrich) was added to the bottle. The mixture was allowed to react for 4 h in a sonication bath, then it was centrifuged at 3500 ***g*** for 30 min. The supernatant was discarded, and the spheres were re-dispersed in 35 mL of ethanol. The spheres were centrifuged again at 1000 ***g*** for 1 h, and the supernatant was discarded. The washing was conducted in three steps. First, the spheres were washed five times with centrifugation at 1500 ***g*** for 15 min and re-dispersing in 35 mL of ethanol (rinses 1, 2, and 5) or ultrapure water (three-stage Millipore Milli-Q plus 185, Billerica, MA) (rinses 3 and 4). Second, the spheres were washed three time with 30 mL of ethanol and centrifugation at 700 ***g*** for 15 min. Third, the spheres were washed seven times with 30 mL of ultrapure water and centrifugation at 700 ***g*** for 15 min. Finally, a stock suspension of spheres was obtained by adding 40 mL of ultrapure water to the precipitate.

Bullet-like silica particles were fabricated using the one-pot method [12,28]. In a plastic bottle, 50 mL of 1-pentanol (99%, Sigma Aldrich) and 5 g of polyvinylpyrrolidone (PVP, molecular weight 40,000, Sigma Aldrich) were added and completely dissolved by sonication for 2 h. Next, 5 mL of absolute ethanol, 1.4 mL of ultrapure water and 0.5 mL of 0.18 M sodium citrate dihydrate (SCD 99%, Sigma Aldrich) were added and mixed by 1 min of agitation by hand. This resulted in an emulsion of water droplets in pentanol stabilized by SCD and PVP. Next, 0.85 mL of ammonia were added followed by 1 min of agitation by hand. After this, 0.25 mL of TEOS were slowly added and the bottle was gently agitated for 30 s. The bottle was left to rest, and the reaction was allowed to proceed for 17 h at 20 °C. The bullet-like particles were collected and washed following the same steps of the spheres. Finally, a stock suspension of bullet-like particles was made by adding 40 mL of ultrapure water to the precipitate.

Detailed procedures to characterize the spherical and bullet-like silica particles are provided in the Supplementary Information (SI). Characterization included FT–IR, N_2-adsorption for the BET surface area and porosity, Scanning Electron Microscopy (SEM), Energy Disperse X-ray Spectroscopy (EDS), Dynamic Light Scattering (DLS) for the size, and zeta potential measurements.

2.2. Particle deposition kinetics

A QCM–D system (Q–Sense Explorer, Biolin Scientific AB, Sweden) was utilized to evaluate the deposition kinetics of spherical and bullet-like silica particles on a 5 MHz AT–cut quartz sensor crystal with a silica-coated surface (QSX 303, Batch 0801110-3, Biolin Scientific AB, Sweden). Sensor cleaning was conducted according to the protocol in the user's guide from the manufacturer. A peristaltic pump (REGLO *Digital* ISM 596, ISMATEC, Switzerland) was utilized to inject the particle suspension in the flow chamber at a flow rate of 0.1 mL/min and the temperature within the chamber was maintained at 25 °C. This flow rate was selected to be consistent with previous literature [29]. Computational fluid dynamics (CFD) simulations of the QCM–D experiment were conducted to assess the flow field and transport behavior of silica colloids. The hydrodynamics inside the QCM–D flow chamber were simulated in three dimensions using multiphase flow equations, and transport was simulated using particle tracking that took into account drag, lift, gravity and electrophoretic forces. Details of these CFD simulations are shown in the SI.

Deposition experiments were conducted in NaCl electrolyte (Sigma-

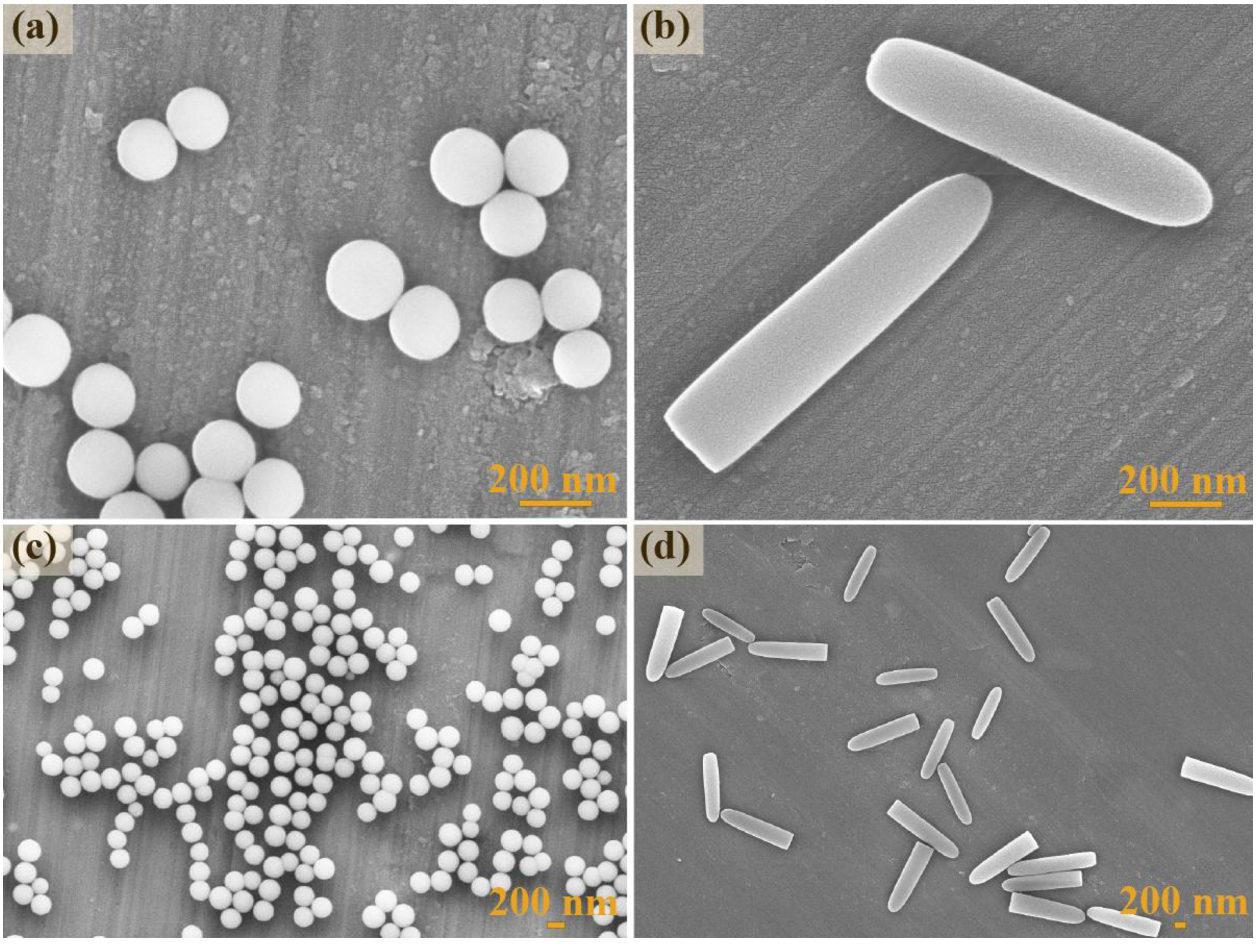

Fig. 1. Representative scanning electron microscope images of diluted samples of (a, c) spherical and (b, d) bullet−like silica particles.

Aldrich) solutions at low ($10^{0.0}$ and $10^{0.5}$ mM), intermediate ($10^{1.0}$ and $10^{1.5}$ mM), and high ($10^{2.0}$ and $10^{2.5}$ mM) IS with an unadjusted pH (5.4–5.7). Monovalent electrolyte was chosen to avoid non-DLVO interactions; e.g., cation bridging in the presence of multi-valent cations. Deionized water was injected until a stable baseline in the third overtone (f_3) was obtained; e.g., ± 0.2 Hz drift over 20 min. Next, the system was equilibrated by injection of particle-free electrolyte solution at a selected IS for 20 min. A particle suspension with a concentration of 100 ppm at the same IS was then injected for 20 min. Finally, particle-free electrolyte solution at the same IS was injected for another 20 min. Additional details pertaining to the QCM–D measurements are given in the SI. The deposition rate (r_d) of silica particles was determined from the slope of the $f_{(3)}$ of QCM–D readings by linear regression analysis.

3. DLVO prediction

In this work we compare four interaction energy models and experimentally verified them to investigate the concept that particle shape does or does not affect deposition. Classical DLVO theory for a particle-plate configuration was utilized to model the deposition of silica particles on a silica surface (QCM–D sensor). It is called classical because total interaction energies between a particle and the surface were quantified as the arithmetic sum of VDW and EDL interactions as a function of separation distance. The four DLVO models that were considered in this work were: (i) the DA method [30,31] which assumes a spherical particle (denoted as DA model); (ii) the SEI [1] method for an equivalent spherical particle (denoted as SEI equivalent sphere); (iii) the SEI approach for an equivalent ellipsoidal particle [2] (denoted as SEI equivalent ellipsoid); and (iv) the SEI approach for an equivalent cylinder or rod particle [25] (denoted as SEI equivalent rod). In contrast to the equivalent sphere approaches, the SEI equivalent ellipsoid and rod models take into account the particle shape and orientation with the surface.

Details pertaining to the DLVO models are provided in the SI. The DA model is used to obtain expressions for the interaction energies through integrations that consist of assumptions about the particle curvature. The consideration of particle shape requires complicated procedures, so it is a common practice to use the DA model to assume

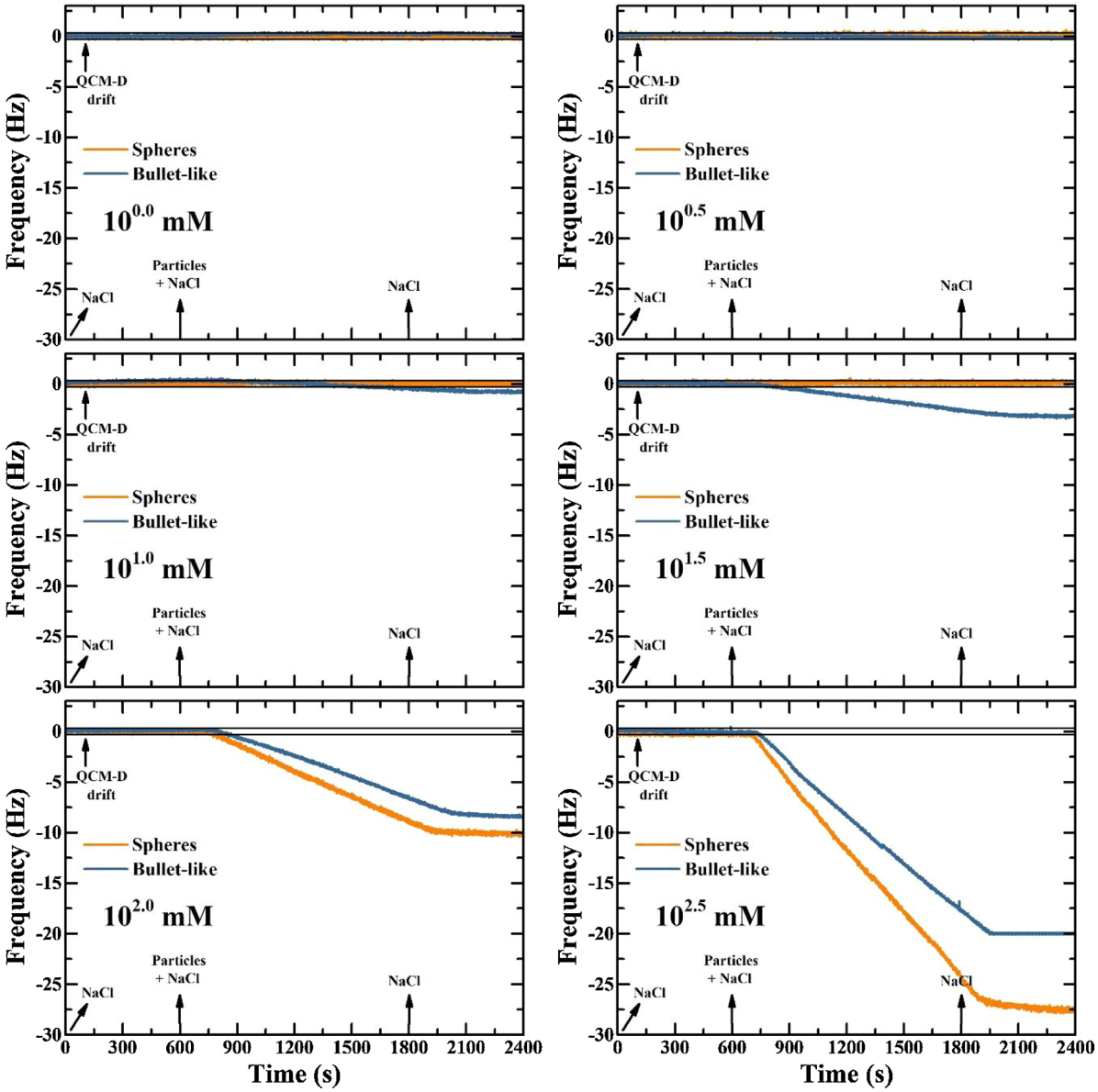

Fig. 2. Representative QCM–D data for deposition experiments with spherical and bullet – like silica particles at unadjusted pH (5.4 – 5.7) when the IS = $10^{0.0}$, $10^{0.5}$, $10^{1.0}$, $10^{1.5}$, $10^{2.0}$, and $10^{2.5}$ mM NaCl. The frequency reported is from the 3rd overtone.

an equivalent sphere. The SEI models consist of integrals that were numerically solved using expressions for non-retarded VDW interaction and the constant surface potential EDL interaction between two flat plates that were given by Hamaker [3,32,33] and Hogg et al. [3,34], respectively. A schematic representing the coordinates for the equivalent rod and ellipsoid models is shown in Figure S1. More details and references for the DA and SEI models are available in the SI.

4. Results and discussion

4.1. Characterization of silica particles

Fig. 1 shows representative SEM images of spherical (Fig. 1a, c) and bullet-like (Fig. 1b, d) silica particles. Particle diameters (D) that were determined from analysis of SEM images were very similar; e.g., D was equal to 214 ± 49 nm and 254 ± 63 nm for spherical and bullet-like particles, respectively. The length (L) and aspect ratio (L/D) for the bullet-like particle were determined from these images to be equal to 1110 ± 182 nm and 5 ± 0.6, respectively. Measurements of the hydrodynamic diameter for spherical and bullet-like silica particles are given in Figure S2a when the IS ranged from $10^{0.0}$ to $10^{2.5}$ mM NaCl. Similar to Fig. 1, hydrodynamics diameters for spherical and bullet-like silica particles equalled 216 ± 5 nm and 1027 ± 71 nm at $10^{0.0}$ mM NaCl, respectively. The hydrodynamic diameters did not change much with the solution IS (Figure S2a), and this indicates that the suspensions were initially stable at different IS.

The chemical composition of the surface of the silica particles were assessed through FT–IR (Figure S3), EDS (Table S1), and zeta potential (Figs. S4 and S5) measurements. The FT–IR peaks at ~1494 and 1425 cm^{-1} correspond [35] to trace impurities from PVP. These peaks in Figure S3 were negligible, and this indicates that our particles do not contain significant PVP on the surface. EDS analysis showed no chemical impurities, and the weight percentages of Si and O of the spherical and bullet-like particles were similar (Table S1). Zeta potentials for spherical and bullet-like silica particles at different pH values were similar and became more negative at higher pH due to formation of silicate ion ($H_3SiO_4^-$) after adsorption of OH^- ions (Figure S4) [36]. The point of zero charge for both particles in Figure S4 is that known for silica. Zeta potentials for spherical and bullet-like silica particles increased (became less negative) with increasing IS due to compression of the double layer (Figure S5). Their values were nearly identical at the lowest and highest IS, but bullet-like particles tended to have higher zeta potentials than spherical particle at intermediate IS (Figure S5). These differences in zeta potential were explicitly included in DLVO calculations discussed in the following sections. It has been reported [37–41] that electrophoretic mobility of a particle can be affected by its shape and orientation, and that shape does not have an influence in the mobility at certain IS conditions. Nevertheless, more discussion on this current knowledge is beyond the scope of our research. Collectively, the above analysis of the chemical composition demonstrated that our silica

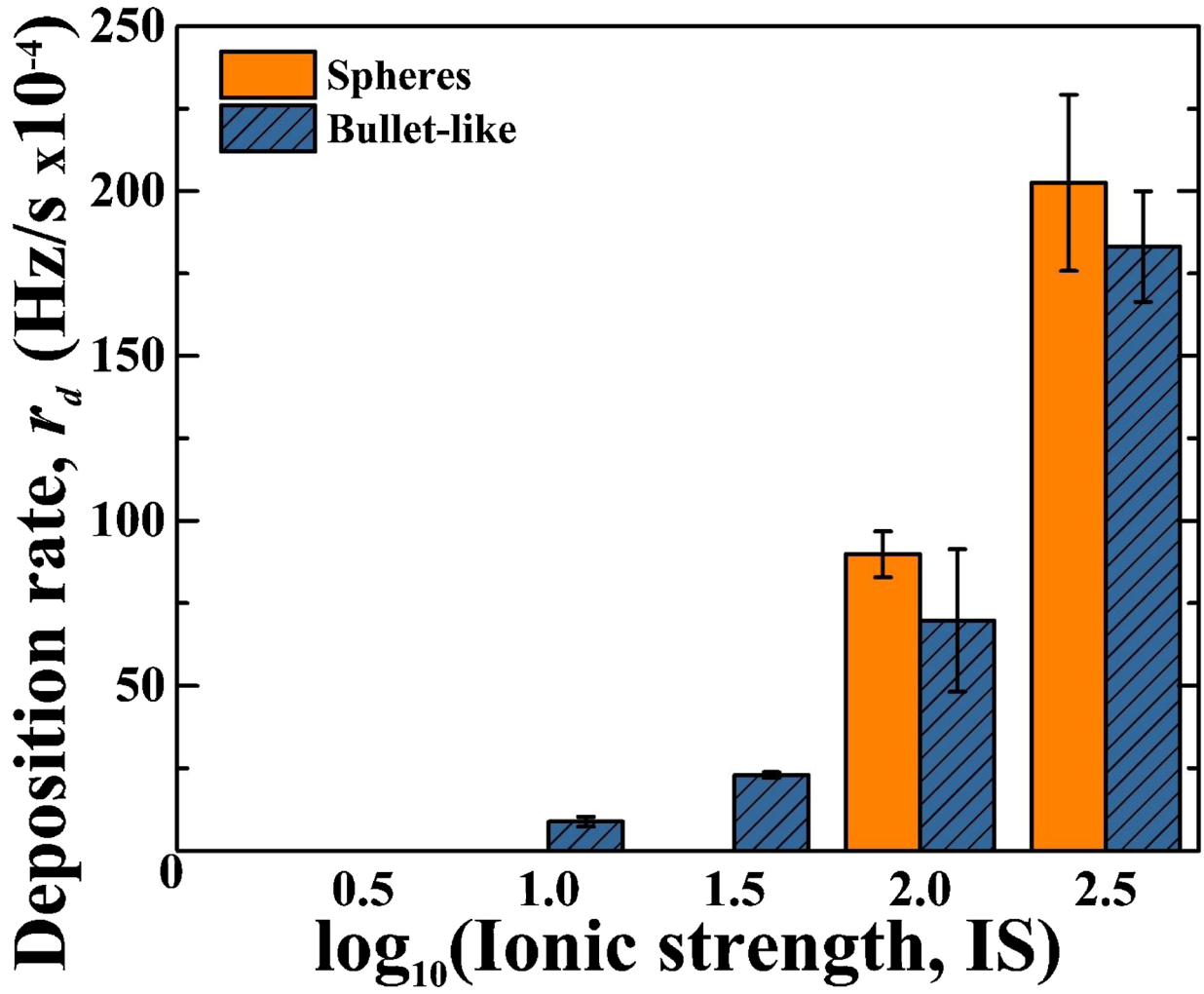

Fig. 3. Deposition rates (r_d) of the silica particles on a silica sensor at unadjusted pH (5.4–5.7) as a function of IS ($n \geq 3$). Rates within drift of the QCM–D frequency reading indicated no conclusive deposition.

particles have a well-defined surface chemistry, are of high purity, and are monodispersed. A detailed information on physicochemical properties of both silica particles can be found in SI.

4.2. QCM − D Experiments

Results of CFD simulations of the QCM–D experiment are shown in Figs. S6 − S9. Simulations demonstrated that flow inside the flow chamber was laminar (low Re number) and that the transport of particles was dominated by convection (high Pe number). Diffusive transport (low Pe number) appeared only at close distances from the walls. In addition, an interesting result from the simulations is that particles do not touch the sensor surface. Thus, if particles do not touch the sensor surface by influence of hydrodynamics, the deposition can be attributed to particles overcoming an energy barrier at close distances from the sensor surface and falling into an attractive energy state next to the sensor surface that can resist the applied hydrodynamic forces and torques.

Fig. 2 presents representative QCM–D data for deposition experiments using spherical and bullet-like silica particles at unadjusted pH (5.4–5.7) when the IS = $10^{0.0}$, $10^{0.5}$, $10^{1.0}$, $10^{1.5}$, $10^{2.0}$, and $10^{2.5}$ mM NaCl. The corresponding values of r_d for these experiments are given in Fig. 3. The r_d of spherical and bullet-like silica particles increased with IS due to compression of the electrical double layer thickness. However, significant r_d only occurred when IS $\geq 10^{2.0}$ mM for spherical particles and when IS $\geq 10^{1.0}$ mM for bullet-like particles. Consequently, deposition occurred over a wider range of IS for bullet-like than spherical particles. The r_d for spherical and bullet-like particles were only similar at the low ($10^{0.0}$ and $10^{0.5}$ mM) and high ($10^{2.0}$ and $10^{2.5}$ mM) IS. This information unequivocally confirms that particle shape plays an important role in deposition, especially at intermediate IS conditions ($10^{1.0}$ and $10^{1.5}$ mM).

It should be mentioned that the hydrodynamic diameter of the bullet-like particles in the QCM–D influent slightly increased during deposition experiments when the IS $\geq 10^{1.0}$ mM (Figure S2b). This suggests slight aggregation of silica particle suspension being injected and it will be discussed briefly later in the manuscript.

4.3. Interaction energies for spherical particles

The total interaction energy profiles between spherical particles and the QCM–D sensor surface were calculated as a function of separation distance using the DA and SEI equivalent sphere models (Table 1 and Fig S10). Deposition of the spherical particles was considered to occur only in a strong primary minimum because the depth of the secondary energy minimum (Table S2 (−0.03 to −3 kT)) was small relative to diffusive and hydrodynamic forces. The QCM–D r_d was therefore related to the calculated energy barriers (EB) for the various DLVO models. In particular, the probability for particles to diffuse over the EB into a primary minimum rapidly increases from 0 to 1 as the EB decreases from around 10 to 0 kT, respectively [42] (where k and T denote the Boltzmann constant and the absolute temperature, respectively). Table 1 provides the EB for the spherical silica particles. Both the DA and SEI equivalent sphere models predict a large EB (conditions unfavorable for deposition) at low and intermediate IS due to electrostatic repulsion. These predictions are consistent with experimental observations in Fig. 3 that show no deposition of spherical silica particles. At high IS the DA and SEI equivalent sphere models predict low or no EB (conditions favorable for deposition) due to compression of the double layer which increases the relative importance of attractive VDW interactions. These predictions are consistent with the experimental results in Fig. 3 that show significant deposition of spherical silica particles.

It has been theoretically reported in the literature [43–45] that the DA model overestimates the interaction energies for small particles (tens of nanometers) at low IS. We did not see considerable differences in the EB height between the DA and SEI equivalent sphere models because the silica spheres in our study are bigger than some tens of nanometers.

4.4. Interaction energies for bullet-like particles

The total interaction energy profiles between bullet-like particles and the QCM–D sensor surface were calculated as a function of separation distance using the DA, SEI equivalent sphere, SEI equivalent ellipsoid, and SEI equivalent rod models. Interaction energy profiles for SEI equivalent rod model at angles of orientation (φ) equal to 0, $\pi/6$, $\pi/4$, and $\pi/2$ rad are given in Figure S11 (e.g., φ is the angle that the larger axis of the particles makes with the element normal to the surface). The figure also shows results from DA and SEI equivalent sphere models. Information on the EB heights for these models are given in Tables 1–3. A summary of the calculated values of the secondary minima for these models is given in Tables S2 − S4 (equivalent sphere models: −0.5 to −8 kT, equivalent ellipsoid: −0.04 to −4 kT, equivalent rod: −0.05 to −16 kT). The depths of the secondary energy minimum were small relative to diffusive and hydrodynamic forces, and deposition of the bullet-like silica particles was therefore only considered to occur in a strong primary minimum when the EB was less than around 10 kT [42]. Consistent with experimental observations in Fig. 3, all of the interaction energy models predict an EB > 10 kT and no deposition at low ($10^{0.0}$ and $10^{0.5}$ mM) IS, and no EB and favorable deposition at high ($10^{2.0}$ and $10^{2.5}$ mM) IS. Consideration of particle shape and orientation was therefore not needed to correctly interpret experimental observations at low and high IS. Conversely, at intermediate ($10^{1.0}$ and $10^{1.5}$ mM) IS the interaction energy models predict differences in the EB height and deposition with the particle shape and orientation. Consistent with experimental observations in Fig. 3, the SEI equivalent ellipsoid and rod models predict that deposition may occur for some particle orientations (e.g., $\varphi = 0$, $\pi/6$ and/or $\pi/4$ rad) that produce an EB < 10 kT. On the other hand, deposition is not predicted when using the DA and SEI equivalent sphere models. An explanation for differences in model predictions at intermediate IS is given below.

The interaction energy depends on the projected surface area of the particle on the QCM–D sensor surface and the separation distance of local surface elements. The DA and SEI equivalent sphere models do not accurately account for the projected surface area and the separation distance of local surface elements when the bullet − like particles are at various φ, and therefore do not correctly describe observed trends in deposition at intermediate IS. The SEI equivalent ellipsoid and rod models predict changes in EB with changes in φ (Tables 2 and 3, respectively). In detail, the SEI equivalent ellipsoid model predicts EB heights in the order $0 < \pi/6 < \pi/4 < < \pi/2$ rad (Table 2) while the SEI equivalent rod model in the order $\pi/4 < \pi/6 < < 0 < \pi/2$ rad

Table 1
Interaction energy barriers between a silica particle and an isotropic planar silica surface (QCM–D sensor) with the ionic strength of NaCl at unadjusted pH (5.4–5.7). The interaction energy was calculated as the sum of van der Waals and electrostatic interactions for a sphere − plate configuration.

Ionic strength (mM)	Energy barrier according to the equivalent sphere models (kT)			
	Derjaguin approximation DLVO		Surface element integration DLVO	
	Sphere	Bullet − like	Sphere	Bullet − like
$10^{0.0}$	191.7	916.5	170.6	895.7
$10^{0.5}$	154.4	640.5	145.2	633.0
$10^{1.0}$	119.9	199.3	115.9	190.3
$10^{1.5}$	37.5	29.3	37.3	27.0
$10^{2.0}$	7.2	NEB[a]	7.7	NEB[a]
$10^{2.5}$	NEB[a]	NEB[a]	NEB[a]	NEB[a]

[a] NEB means no energy barrier.

Table 2
Interaction energy barriers between a bullet – like silica particle and an isotropic planar silica surface (QCM–D sensor) with the ionic strength of NaCl at unadjusted pH (5.4–5.7), and at four angles of interaction during deposition. The interaction energy was calculated as the sum of van der Waals and electrostatic interactions for an ellipsoid – plate configuration.

Ionic strength (mM)	Energy barrier according to the surface element integration DLVO equivalent ellipsoid (kT)			
	φ[b] = 0	π/6	π/4	π/2
$10^{0.0}$	52.7	53.8	56.1	512.1
$10^{0.5}$	34.6	35.2	36.5	405.8
$10^{1.0}$	10.7	10.8	11.2	147.4
$10^{1.5}$	1.4	1.5	1.5	27.9
$10^{2.0}$	NEB[a]	NEB[a]	NEB[a]	NEB[a]
$10^{2.5}$	NEB[a]	NEB[a]	NEB[a]	NEB[a]

[a] NEB means no energy barrier.
[b] Angle of interaction is in radians.

Table 3
Interaction energy barriers between a bullet – like silica particle and an isotropic planar silica surface (QCM–D sensor) with the ionic strength of NaCl at unadjusted pH (5.4–5.7), and at four angles of interaction during deposition. The interaction energy was calculated as the sum of van der Waals and electrostatic interactions for a rod – plate configuration.

Ionic strength (mM)	Energy barrier according to the surface element integration DLVO equivalent rod (kT)			
	φ[b] = 0	π/6	π/4	π/2
$10^{0.0}$	926.3	89.1	66.3	2231.7
$10^{0.5}$	1050.1	46.7	34.3	1947.8
$10^{1.0}$	567.5	11.9	8.6	820.2
$10^{1.5}$	190.5	0.7	0.4	206.2
$10^{2.0}$	NEB[a]	NEB[a]	NEB[a]	NEB[a]
$10^{2.5}$	NEB[a]	NEB[a]	NEB[a]	NEB[a]

[a] NEB means no energy barrier.
[b] Angle of interaction is in radians.

(Table 3). Differences in the geometry of ellipsoid and rod models (projected area and separation distances for local surface elements) cause variations in predicted EBs. In addition, the EB can be slightly smaller due to real fluctuations in particle energy, particle diffusion, employed surface charge boundary and/or numerical integration method. Accordingly, the SEI equivalent ellipsoid model predicts that deposition can occur when $\varphi = 0$, π/6, π/4 rad at intermediate ($10^{1.0}$ and $10^{1.5}$ mM) IS and the SEI equivalent rod model predicts deposition when $\varphi = \pi/6$ and π/4 rad. In the case of the rod model, the same trend has been previously reported for solid rods having low aspect ratios ($2 <$ aspect ratio < 25) [26]. The contribution of the circular end of the rod that is closest to the sensor surface is larger than that from the side surface when $0 \leq \varphi \leq \pi/4$ rad. An increase in φ and/or the local element separation distance decreases the interaction area of the end surface resulting in a net reduction on the interaction energy [26]. Previous research has reported that the EB for a hollow cylinder gradually increased when φincreased from 0 to π/2 rad [25]. However, that research considered a different geometry with very high aspect ratios (e.g., non – modified and surface – modified single walled hollow carbon nanotubes), a hollow interior, and different surface chemistry.

The value of φ manipulates the separation distance between local elements on the surface of the bullet – like silica particles and the sensor surface. Consequently, this changes the strength of both VDW and EDL interactions. The EBs in Tables 2 and 3(SEI equivalent ellipsoid and rod model, respectively) reflect changes in the relative importance of EDL repulsion and VDW attraction with IS. There is no EB at high IS for all φ because the reduction in the EDL repulsion causes the VDW attraction to be dominant. At low IS, the SEI equivalent ellipsoid and rod models predicted that changes in the EB height with φ are not sufficient to allow deposition. That also indicates the prescence of strong EDL repulsions. At intermediate IS the two models differently predicted the EB allowing bullet – like silica particle deposition. The SEI equivalent ellipsoid model predicts deposition with changes in φ at intermediate IS (Table 2). Nevertheless, the EB is high when $\varphi = \pi/2$ rad indicating the presence of strong EDL repulsions, and thus, this angle is not energetically favorable for particle deposition. The SEI equivalent rod model (Table 3) predicts high EBs at intermediate IS when $\varphi = 0$ and π/2 rad, indicating the presence of strong EDL repulsions. High EBs predict that the bullet – like silica particles will not deposit on the sensor suface. However, deposition can occur when $\varphi = \pi/6$ and π/4 rad.

Therefore, the predictions from the SEI equivalent ellipsoid and rod models are consistent with experimental observations for bullet – like particles in Fig. 3 at low, high, and intermediate IS. At intermediate IS, the observed deposition of bullet – like particles suggests that these particles likely find orientations (e.g., $\varphi = 0$—π/4 rad or π/6—π/4 rad depending on geometry) that minimize the repulsive interactions and overcome the EB; this is represented in a diagram in Fig. 4. According to Tables 2 and 3, values of the EB at intermediate ($10^{1.0}$ and $10^{1.5}$ mM) IS are small and relatively close (0.4–12 kT) when $\varphi = 0$, π/6 and π/4 rad for ellipsoid, and π/6 and π/4 rad for rod. Accordingly, the SEI equivalent ellipsoid and rod models can successful interpret the deposition rates in Fig. 3 for bullet – like silica particles at intermediate IS. A graphical summary of all the predicted trends of EB as a function of φ and solution IS is shown in Fig. 5 for the SEI equivalent ellipsoid and rod models.

It should be mentioned that the hydrodynamic diameter of the bullet – like silica particles slightly increased during injection with increasing IS (Figure S2). This implies that the bullet–like particles exhibited minor aggregation during injection. The above deposition results (Fig. 3–5) for SEI DLVO ellipsoid and rod models suggest that aggregation will likely be influenced by particle shape and orientation. A previous study [4] has also reported an effect of particle shape on aggregation of silica particles. Nevertheless, minor aggregation of the bullet – like silica particles did not have an apparent influence on r_d in Fig. 2, and these results could be successfully interpreted using predicted EBs from SEI DLVO equivalent ellipsoid and rod models (Tables 2 and 3). More research on aggregation and deposition of non – spherical particles/aggregates is warranted, but that is beyond the scope of this study.

McNew et al. [21] reported that the deposition of spherical polystyrene particles on humic acid (HA) coated silica surfaces was higher than that of ellipsoidal polystyrene particles when the IS was lower than $10^{2.0}$ mM NaCl, whereas the deposition of both particles was practically the same on alginate coated surfaces. An agreement between DLVO predictions and experiments was only found for the deposition of ellipsoidal polystyrene on HA coated surfaces and for both spherical and ellipsoidal polystyrene on alginate coated surfaces. The enhanced deposition of spherical polystyrene particles on HA coated surfaces was attributed to higher surface roughness or steric (entanglement) effects. In contrast, other studies suggest that HA should cause electrosteric repulsion that inhibits deposition [46,47]. Consequently, a fundamental understanding of the influence of particle shape and orientation on deposition has previously been hindered by confounding effects from non – DLVO interactions. Our study clearly identified the effect of particle shape and orientation at intermediate IS because we eliminated the interference from non – DLVO interactions. In addition, Liu et al. [5] conducted column experiments to investigate the effect of shape on the transport of polystyrene particles in porous media. A comparison between their work and our work is not straightforward because they used a system causing many possible mechanisms (attachment, straining, etc.) for particle retention in porous media. Also, they did not consider the exact particle geometry in DLVO calculations based on the DA. Nevertheless, they concluded that questions remain on the particle orientations relative to the collector, and our study addressed that

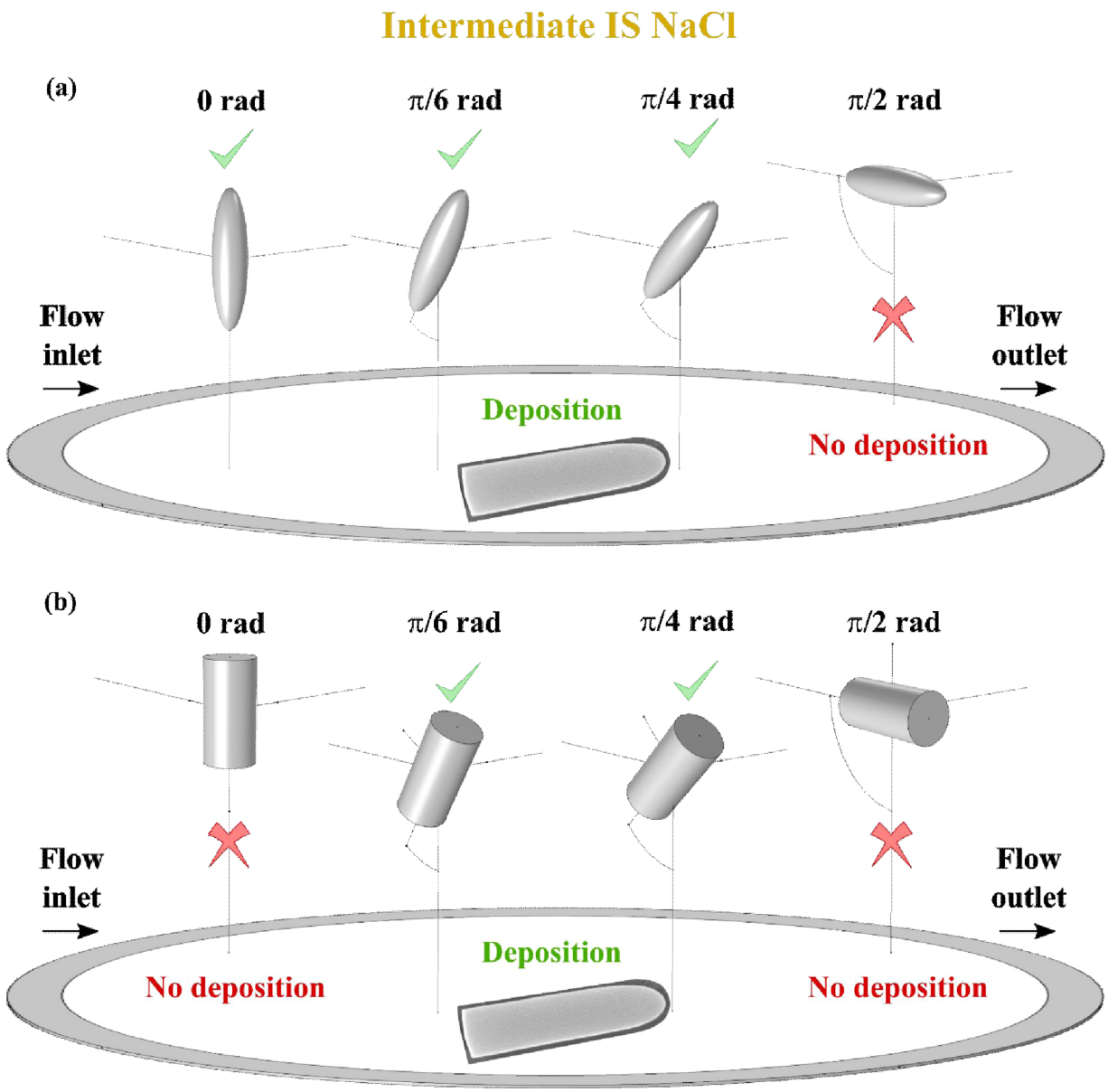

Fig. 4. Diagram of the estimated angles of deposition at intermediate IS according to the SEI DLVO equivalent (a) ellipsoid and (b) rod models.

question by considering several orientations of bare rod−like silica particles in DLVO calculations.

5. Conclusions

The DA and SEI equivalent sphere models predicted the deposition behavior of spherical silica particles on a QCM–D silica sensor when the IS = $10^{0.0}$, $10^{0.5}$, $10^{1.0}$, $10^{1.5}$, $10^{2.0}$, and $10^{2.5}$ mM NaCl during laminar flow and convective transport. Similarly, the DA, SEI equivalent sphere, and SEI equivalent ellipsoid and rod models were able to correctly predict the deposition behavior of bullet−like silica particles at low IS ($10^{0.0}$ and $10^{0.5}$ mM) or high ($10^{2.0}$ and $10^{2.5}$ mM) IS of NaCl when the EB clearly predicted unfavorable and favorable conditions for deposition, respectively. This suggests that the bullet−like silica particles can be treated either as equivalent spheres, ellipsoids or rods at low and high IS. Conversely, the DA and SEI equivalent sphere models were not able to predict the deposition behavior of bullet−like silica particles under intermediate IS ($10^{1.0}$ and $10^{1.5}$ mM) conditions. This failure suggests that the use of these models in this range of IS can lead to incorrect predictions.

Only the SEI equivalent ellipsoid and rod models successfully predicted the deposition behavior of bullet−like silica particles under all (low, intermediate, and high) IS conditions. In particular, these models predicted that the bullet−like silica particles can deposit on a “smooth” silica surface under intermediate IS conditions when the angle of interaction ranged from 0 to π/4 rad (φ = 0, π/6 and π/4 rad for ellipsoid, and π/6 and π/4 rad for rod). These angles were able to reduce the EB sufficiently to create conditions that were energetically favorable for deposition. The bullet−like silica particles apparently move to less convective regions as they approach the silica surface and diffusion changes the angle of interaction until an *energetically favorable angle for deposition* is achieved. In fact, dynamic rotation and translation of rod−like silica particles due to diffusion have been measured using a holographic microscopy [48]. The use of the SEI equivalent ellipsoid and rod models is therefore enthusiastically encouraged to predict the interaction energies of bullet−like silica particles.

Until now, the effect of shape was reported in the presence of non−DLVO interactions due to residual PVA on polystyrene particles. Our study was the first to systematically examine the deposition of bullet−like silica particles with a well−defined surface chemistry

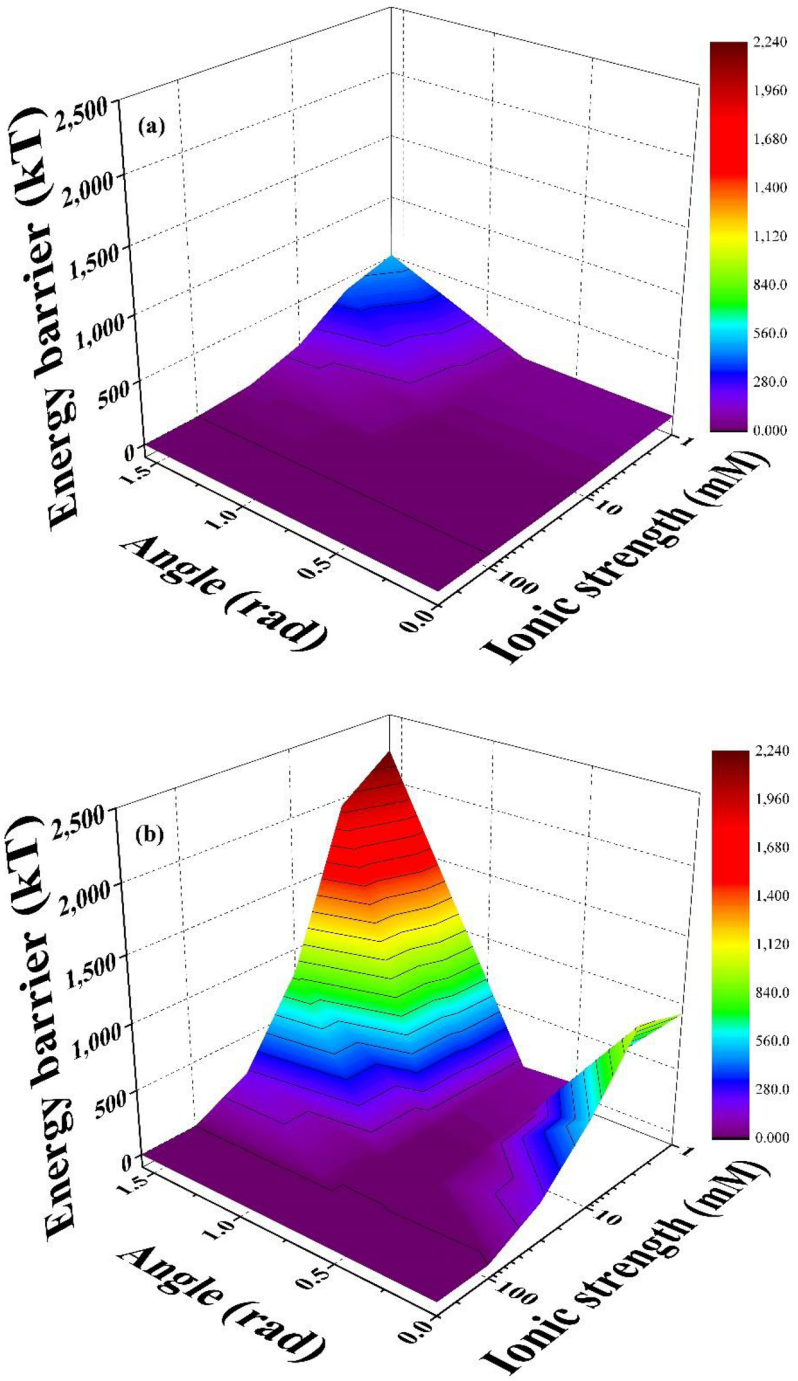

Fig. 5. Surface plot of the predictions of interaction energy barriers between a bullet – like silica particle and an isotropic planar silica surface (QCM–D sensor) as a function of the solution IS and the orientation angle of interaction. The interactions were predicted for (a) ellipsoid–plate and (b) rod–plate configurations in monovalent salt (NaCl) at unadjusted pH (5.4–5.7).

under various IS conditions in a system with a uniform flow field. These results were interpreted using interaction energy calculations that considered various particle shapes and orientations. It has been experimentally shown that the shape of silica particles had an effect on deposition on smooth silica surfaces at intermediate IS of $10^{1.0}$ and $10^{1.5}$ mM NaCl. In these cases, particle shape and orientation must be accurately considered in the interaction energy calculations to correctly predict observed deposition behavior. Interestingly, these two identified IS are frequently observed in many applications such as human blood [49–51], animal blood [51], or transport of bacteria [52] or colloids [53].

CRediT authorship contribution statement

Allan Gomez-Flores: Methodology, Investigation, Software, Writing - original draft. **Scott A. Bradford:** Writing - review & editing. **Gukhwa Hwang:** Writing - review & editing. **Sowon Choi:** Writing - review & editing. **Meiping Tong:** Writing - review & editing. **Hyunjung Kim:** Conceptualization, Supervision, Writing - review & editing.

Declaration of Competing Interest

The authors declare no conflicts of interest.

Acknowledgments

The authors acknowledge support from the Basic Science Research Program through the National Research Foundation of Korea (NRF) funded by the Ministry of Education (NRF-2015R1D1A3A01020766), and the Korea Energy and Mineral Resources Engineering Program (KEMREP). The authors greatly thank Dr. Brendan Headd at the US Salinity Laboratory of the USDA for conducting zeta potential measurements.

Appendix A. Supplementary data

Supplementary material related to this article can be found, in the online version, at doi:https://doi.org/10.1016/j.colsurfa.2020.124921.

References

[1] S. Bhattacharjee, M. Elimelech, Surface element integration: a novel technique for evaluation of DLVO interaction between a particle and a flat plate, J. Colloid Interface Sci. 193 (1997) 273–285.
[2] S. Bhattacharjee, J.Y. Chen, M. Elimelech, DLVO interaction energy between spheroidal particles and a fiat surface, Colloids Surf. A Physicochem. Eng. Asp. 165 (2000) 143–156.
[3] J.N. Israelachvili, Intermolecular and Surface Forces, 3rd ed., Academic Press, Burlington, Mass, 2011.
[4] L. Wu, C.P. Ortiz, D.J. Jerolmack, Aggregation of elongated colloids in water, Langmuir 33 (2017) 622–629.
[5] Q. Liu, V. Lazouskaya, Q.X. He, Y. Jin, Effect of particle shape on colloid retention and release in saturated porous media, J. Environ. Qual. 39 (2010) 500–508.
[6] T. Knappenberger, S. Aramrak, M. Flury, Transport of barrel and spherical shaped colloids in unsaturated porous media, J. Contam. Hydrol. 180 (2015) 69–79.
[7] M.B. Salerno, M. Flamm, B.E. Logan, D. Velegol, Transport of rodlike colloids through packed beds, Environ. Sci. Technol. 40 (2006) 6336–6340.
[8] M.B. Seymour, G.X. Chen, C.M. Su, Y.S. Li, Transport and retention of colloids in porous media: does shape really matter? Environ. Sci. Technol. 47 (2013) 8391–8398.
[9] J.E. Saiers, J.N. Ryan, Colloid deposition on non-ideal porous media: the influences of collector shape and roughness on the single-collector efficiency, Geophys. Res. Lett. 32 (2005).
[10] S. Sacanna, D.J. Pine, G.R. Yi, Engineering shape: the novel geometries of colloidal self-assembly, Soft Matter 9 (2013) 8096–8106.
[11] P. Kolhar, A.C. Anselmo, V. Gupta, K. Pant, B. Prabhakarpandian, E. Ruoslahti, S. Mitragotri, Using shape effects to target antibody-coated nanoparticles to lung and brain endothelium, Proc. Natl. Acad. Sci. USA 110 (2013) 10753–10758.
[12] M. Fu, K. Chaudhary, J.G. Lange, H.S. Kim, J.J. Juarez, J.A. Lewis, P.V. Braun, Anisotropic colloidal templating of 3D ceramic, semiconducting, metallic, and polymeric architectures, Adv. Mater. 26 (2014) 1740–1745.
[13] W.L. Li, K. Lu, J.Y. Walz, M. Anderson, Effects of rod-like particles on the microstructure and strength of porous silica nanoparticle composites, J. Am. Ceram. Soc. 96 (2013) 398–406.
[14] J. He, B.Y. Yu, M.J. Hourwitz, Y.J. Liu, M.T. Perez, J. Yang, Z.H. Nie, Wet-chemical synthesis of amphiphilic rodlike silica particles and their molecular mimetic assembly in selective solvents, Angew. Chem. Int. Ed. English 51 (2012) 3628–3633.
[15] P.T.L. Koh, F.P. Hao, L.K. Smith, T.T. Chau, W.J. Bruckard, The effect of particle shape and hydrophobicity in flotation, Int. J. Miner. Process. 93 (2009) 128–134.
[16] D.I. Verrelli, W.J. Bruckard, P.T.L. Koh, M.P. Schwarz, B. Follink, Particle shape effects in flotation. Part 1: Microscale experimental observations, Miner. Eng. 58 (2014) 80–89.
[17] T.G. Vizcarra, S.L. Harmer, E.M. Wightman, N.W. Johnson, E.V. Manlapig, The influence of particle shape properties and associated surface chemistry on the flotation kinetics of chalcopyrite, Miner. Eng. 24 (2011) 807–816.
[18] S. Cooper, M.W. Denny, A conjecture on the relationship of bacterial shape to motility in rod-shaped bacteria, FEMS Microbiol. Lett. 148 (1997) 227–231.
[19] A.R.M.N. Afrooz, S.T. Sivalapalan, C.J. Murphy, S.M. Hussain, J.J. Schlager, N.B. Saleh, Spheres vs. rods: the shape of gold nanoparticles influences aggregation and deposition behavior, Chemosphere 91 (2013) 93–98.
[20] S. Aramrak, M. Flury, J.B. Harsh, R.L. Zollars, H.P. Davis, Does colloid shape affect detachment of colloids by a moving air-water interface? Langmuir 29 (2013) 5770–5780.
[21] C.P. McNew, N. Kananizadeh, Y.S. Li, E.J. LeBoeuf, The attachment of colloidal particles to environmentally relevant surfaces and the effect of particle shape, Chemosphere 168 (2017) 65–79.
[22] C.C. Ho, A. Keller, J.A. Odell, R.H. Ottewill, Monodisperse ellipsoidal polystyrene latex-particles - preparation and characterization, Polym. Int. 30 (1993) 207–211.
[23] L. Florez, C. Herrmann, J.M. Cramer, C.P. Hauser, K. Koynov, K. Landfester, D. Crespy, V. Mailander, How shape influences uptake: interactions of anisotropic polymer nanoparticles and human mesenchymal stem cells, Small 8 (2012) 2222–2230.
[24] J. Hong, C.K. Hong, S.E. Shim, Synthesis of polystyrene microspheres by dispersion polymerization using poly(vinyl alcohol) as a steric stabilizer in aqueous alcohol media, Colloids Surf. A Physicochem. Eng. Asp. 302 (2007) 225–233.
[25] L. Wu, B. Gao, Y. Tian, R. Munoz-Carpena, K.J. Zigler, DLVO interactions of carbon nanotubes with isotropic planar surfaces, Langmuir 29 (2013) 3976–3988.
[26] A. Gomez-Flores, S.A. Bradford, L. Wu, H. Kim, Interaction energies for hollow and solid cylinders: role of aspect ratio and particle orientation, Colloids Surf. A Physicochem. Eng. Asp. 580 (2019) 123781.
[27] W. Stober, A. Fink, E. Bohn, Controlled growth of monodisperse silica spheres in micron size range, J Colloid InterfSci 26 (1968) 62–69.
[28] A. Kuijk, A. Imhof, M.H.W. Verkuijlen, T.H. Besseling, E.R.H. van Eck, A. van Blaaderen, Colloidal silica rods: material properties and fluorescent labeling, Part. Part. Syst. Charact. 31 (2014) 706–713.
[29] M.P. Tong, P.T. Zhu, X.J. Jiang, H. Kim, Influence of natural organic matter on the deposition kinetics of extracellular polymeric substances (EPS) on silica, Colloids Surf. B Biointerfaces 87 (2011) 151–158.
[30] B. Derjaguin, Untersuchungen über die Reibung und Adhäsion, IV, KolloidZeitschrift 69 (1934) 155–164.
[31] L.R. White, On the deryaguin approximation for the interaction of macrobodies, J. Colloid Interface Sci. 95 (1983) 286–288.
[32] H.C. Hamaker, The London—van der Waals attraction between spherical particles, Physica 4 (1937) 1058–1072.
[33] M. Elimelech, Particle Deposition and Aggregation : Measurement, Modelling, and Simulation, Butterworth-Heinemann, Oxford England; Boston, 1995.
[34] R. Hogg, T.W. Healy, D.W. Fuerstenau, Mutual coagulation of colloidal dispersions, Trans. Faraday Soc. 62 (1966) 1638–1651.
[35] M.M. Naiini, M. Ghahari, M.S. Afarani, Synthesis of hollow tadpole like silica particles, Part. Sci. Technol. (2015) null-null.
[36] R.K. Iler, The Chemistry of Silica : Solubility, Polymerization, Colloid and Surface Properties, and Biochemistry, Wiley, New York, 1979.
[37] B.J. Yoon, S. Kim, Electrophoresis of spheroidal particles, J. Colloid Interface Sci. 128 (1989) 275–288.
[38] P.D. Grossman, D.S. Soane, Orientation effects on the electrophoretic mobility of rod-shaped molecules in free solution, Anal. Chem. 62 (1990) 1592–1596.
[39] Y. Solomentsev, J.L. Anderson, Electrophoresis of slender particles, J. Fluid Mech. 279 (1994) 197–215.
[40] H. Ohshima, Henry's function for electrophoresis of a cylindrical colloidal particle, J. Colloid Interface Sci. 180 (1996) 299–301.
[41] H.E. Bakker, T.H. Besseling, J.E.G.J. Wijnhoven, P.H. Helfferich, A. van Blaaderen, A. Imhof, Microelectrophoresis of silica rods using confocal microscopy, Langmuir 33 (2017) 881–890.
[42] W.P. Johnson, Mechanisms of Retention of Biological and Non-biological Colloids in Porous Media, Microbial Surfaces, American Chemical Society, 2008, pp. 297–339.
[43] S. Bhattacharjee, M. Elimelech, M. Borkovec, DLVO interaction between colloidal particles: beyond Derjaguin's approximation, Croat. Chem. Acta 71 (1998) 883–903.
[44] Z. Adamczyk, P. Weronski, Application of the DLVO theory for particle deposition problems, Adv. Colloid Interface Sci. 83 (1999) 137–226.
[45] B.A. Todd, S.J. Eppell, Probing the limits of the Derjaguin approximation with scanning force microscopy, Langmuir 20 (2004) 4892–4897.
[46] T. Phenrat, J.E. Song, C.M. Cisneros, D.P. Schoenfelder, R.D. Tilton, G.V. Lowry, Estimating attachment of nano- and submicrometer-particles coated with organic macromolecules in porous media: development of an empirical model, Environ. Sci. Technol. 44 (2010) 4531–4538.
[47] K.M. Sirk, N.B. Saleh, T. Phenrat, H.J. Kim, B. Dufour, J. Ok, P.L. Golas, K. Matyjaszewski, G.V. Lowry, R.D. Tilton, Effect of adsorbed polyelectrolytes on nanoscale zero valent Iron particle attachment to soil surface models, Environ. Sci. Technol. 43 (2009) 3803–3808.
[48] A. Wang, T.G. Dimiduk, J. Fung, S. Razavi, I. Kretzschmar, K. Chaudhary, V.N. Manoharan, Using the discrete dipole approximation and holographic microscopy to measure rotational dynamics of non-spherical colloidal particles, J. Quant. Spectrosc. Radiat. Transf. 146 (2014) 499–509.
[49] T.C.S. Hsu, J. Steinberg, R. Ledoux, A. Sawitsky, Low ionic-strength reaction of human-blood - relationship between the binding of serum immunoglobulin and complement to red blood-cells and surface-charge of the cells, Br. J. Haematol. 42 (1979) 403–415.
[50] M. Rasia, A. Bollini, Red blood cell shape as a function of medium's ionic strength and pH, BBA 1372 (1998) 198–204.
[51] M.F. Mouat, K.L. Manchester, The intracellular ionic strength of red cells and the influence of complex formation, Comp. Haematol. Int. 8 (1998) 58–60.
[52] H.N. Kim, S.A. Bradford, S.L. Walker, Escherichia coli O157:H7 transport in saturated porous media: role of solution chemistry and surface macromolecules, Environ. Sci. Technol. 43 (2009) 4340–4347.
[53] S.A. Bradford, H.N. Kim, B.Z. Haznedaroglu, S. Torkzaban, S.L. Walker, Coupled factors influencing concentration-dependent colloid transport and retention in saturated porous media, Environ. Sci. Technol. 43 (2009) 6996–7002.